

A comparative study of the effects of constructional elements on the mechanical behaviour of dragonfly wings

H. Rajabi^{1,2} · M. Rezasefat² · A. Darvizeh² · J.-H. Dirks³ · Sh. Eshghi⁴ · A. Shafiei⁴ · T. Mirzababaei Mostofi² · S. N. Gorb¹

Received: 16 December 2015 / Accepted: 16 December 2015 / Published online: 23 December 2015
© Springer-Verlag Berlin Heidelberg 2015

Abstract Although wings of insects show a large variation in morphology, they are all made from a network of irregular veins interconnected through membranous areas. Depending on their shape, size, and position, wing veins are usually divided into three different groups: longitudinal veins, cross-veins and ambient veins. The veins together with the membrane and some other elements such as spines, nodus and pterostigma can be considered as the wing's "constructional elements". In spite of rather extensive literature on dragonfly wing structure, the role of each of these elements in determining the wing's function remains mostly unknown. As this question is difficult to answer in vivo using biomechanical experiments on actual wings, this study was undertaken to reveal the effects of the constructional elements on the mechanical behaviour of dragonfly wings by applying numerical simulations. An image processing technique was used to develop 12 finite element models of the insect wings with different constructional elements. The mechanical behaviour of these models was then simulated under normal and shear stresses due to

tension, bending and torsion. A free vibration analysis was also performed to determine the resonant frequencies and the mode shapes of the models. For the first time, a quantitative comparison was carried out between the mechanical effects selectively caused by different elements. Our results suggest that the complex interactions of veins, membranes and corrugations may considerably affect the dynamic deformation of the insect wings during flight.

1 Introduction

Dragonflies are known as one of the most proficient flyers of the world [3, 17, 22, 36]. They exhibit versatile flight capabilities, which are very difficult to achieve in man-made flying systems. Superior manoeuvre abilities [16, 36], variety of flight styles [44], generation of high lift forces [1], ability of sidewise and backward motions [12] are a few striking characteristics of their flapping flight.

Wings, as the main parts of the insect flight system, have to withstand a high level of mechanical stresses during flight. Given the repeated flapping motion of most insect wings, external loads are mostly applied to the wings in a cyclic manner. Hence, the wings should have a great ability to reduce fatigue related damage effects. The authors, who previously studied dragonfly and locust wings, showed that, up to the fracture point, the wings typically behave similar to brittle materials which may be highly sensitive to stress concentration [9, 10, 13, 29, 31]. Then the question is that how do insect wings cope with the different types of mechanical stresses during flight?

The influence of wing morphology on its aerodynamic performance has been previously investigated by many researchers [7, 19, 20, 28, 42]. It has been shown that

Electronic supplementary material The online version of this article (doi:10.1007/s00339-015-9557-6) contains supplementary material, which is available to authorized users.

✉ H. Rajabi
harajabi@hotmail.com; hrajabi@zoologie.uni-kiel.de

¹ Functional Morphology and Biomechanics, Institute of Zoology, Kiel University, Kiel, Germany

² Department of Mechanical Engineering, The University of Guilan, Rasht, Iran

³ Department of New Materials and Biosystems, Max Planck Institute for Intelligent Systems, Stuttgart, Germany

⁴ Young Researchers and Elite Club, Lahijan Branch, Islamic Azad University, Lahijan, Iran

corrugations have an important role in increasing the torsional rigidity of insect wings [35, 41]. Corrugations also provide enhanced bending rigidity across the wing span [45]. Wootton et al. showed that membranes, during bending, contribute to the overall rigidity of the wing structure [26, 46]. Some researchers indicated that thick veins at the base and the leading edge make the wing stiffer in these parts than the other regions [6, 7, 39]. However, how important are different wing components in relation to each other? How do these constructional elements contribute to the specific mechanical behaviour of wings? How does the mechanical behaviour change, if we remove one of these elements from the wing?

The above questions cannot be addressed experimentally, and thus we need numerical simulations to find the answers. In absence of a thorough quantitative study, this article is the first systematic numerical investigation of the effect of dragonfly wing structure on its free vibration behaviour and load-bearing capacity. Here, we develop a series of finite element (FE) models which contain different constructional elements. These models give us the opportunity to study the effect of each single element separately. It is also important to note that the expression “constructional element” is used here to refer the wing corrugations, longitudinal veins (Fig. 1c, g), cross-veins (Fig. 1d, h), ambient veins (Fig. 1e, i) and membranes (Fig. 1f, j). The results of this study, in particular, the relatively simple numerical models, may help to gain a better insight into the complex biomechanical behaviour of insect wings.

2 Materials and methods

2.1 Modelling procedure

A new FE modelling method has been recently proposed by the authors to develop numerical models of planar

biological structure [15, 31]. The advantage of this method, in comparison with the other available modelling techniques, is the accuracy of the developed models, as well as the short run-time (a few seconds). In this study, we now apply this technique to develop FE models of dragonfly wings. The method, which is based on a digital image processing technique, was implemented in a MATLAB code and is able to develop FE models of complex biological structures. The only required input for the programme is a 2D image representing the desired morphological wing structure. Here, two images of the dragonfly *Orthetrum sabina* (Anisoptera, Libellulidae) fore- and hind-wings are used as the inputs (Fig. 1a, b). In the first step, the programme converts the input image to a binary format where veins and membranes are represented by black and white pixels, respectively. By connecting a specific number of black pixels, which determines the element size, the first element of the model is made. This process is continued until a meshed model of all veins is developed. The number of pixels that makes an element is determined by the user and defines the mesh size. The same process is applied to develop FE models of the white pixels that are surrounded by the black ones. These white pixels represent the membrane of the insect wing. In this way, veins and membrane are modelled separately. At the end, the programme assembles these different parts and develops an integrated model of the wing.

2.2 Out-of-plane modelling

Dragonfly wings are corrugated in both spanwise and chordwise directions. These corrugations may have an important influence on the mechanical behaviour of the insect wing [20, 41]. The described modelling programme, mentioned in the previous section, is also able to model such corrugations. For this purpose, it is necessary to

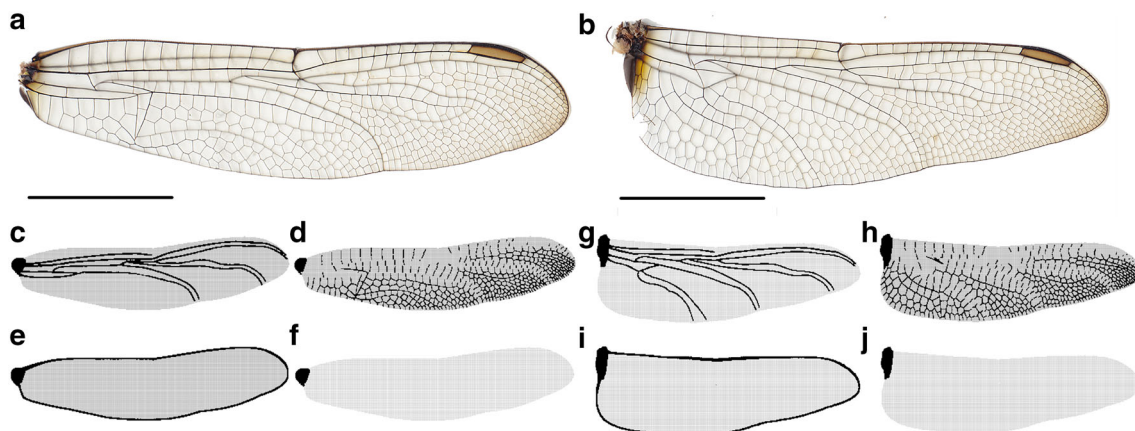


Fig. 1 Right **a** fore- and **b** hind-wings of *Orthetrum sabina* (Anisoptera, Libellulidae) (scale bar 1 cm). Constructional elements of fore- and hind-wings including **c**, **g** longitudinal veins, **d**, **h** cross-veins, **e**, **i** ambient veins, and **f**, **j** membranes

directly assign the heights of some specific nodes. These nodes are the points with the maximum height, and usually along the longitudinal veins on the upper side of the wing. In order to obtain the coordinates of the nodes with maximum height, six fresh dragonfly wings (three forewings and three hind-wings of *Orthetrum sabina* (Anisoptera, Libellulidae), were used. First, they were completely embedded in epoxy resin. The embedded wing samples were then transversally cut into sections of 2–3 mm length with a razor blade. These slices were observed under a light microscope, and the heights of the desired nodes were carefully measured with respect to a predefined coordinate system. Here, to improve the accuracy of our model, we measured the height of more than 60 points. The coordinates of the nodes and their corresponding heights were directly given to the programme. Finally, an averaging technique is used to provide a smooth transition between the nodes with minimum and maximum height values.

The output of the code is a text file that is written in ANSYS parametric design language (APDL) and contains the location of all nodes on the insect wing model and their connections (see suppl. files 1 and 2). The generated text file can be easily exported to any FE commercial software package, such as ANSYS, ABAQUS. Here, we used ABAQUS 6.10 finite element solver to analyse the mechanical behaviour of the developed model under different conditions.

2.3 Numerical models

Twelve FE models of dragonfly wings (six models of forewing and six models of hind-wing) were developed in this paper (Fig. 2). All forewing models have a maximum length of 38.12 mm and a maximum width of 9.11 mm. The length and width of hind-wing models are 36.19 and 11.54 mm, respectively. Four-node shell elements (S4R) with reduced integration and a large-strain formulation were used to represent different components of the models. Each model has a series of specific constructional elements that allow it to be distinguished from the other models. These models with different features allowed us to study the effect of each constructional element on the mechanical behaviour of insect wings under various loading conditions. The detailed characteristics of the models are listed in Table 1, with models of the front wing labelled F and hind-wing H, respectively. Corresponding models have the same indices. As seen in the table, models F1 and H1 are the exact models of the forewing and hind-wing including membrane, all veins and corrugations. The APDL files of these two models have been added as supplementary materials (see suppl. files 1 and 2). The other wing models are developed by excluding the constructional elements from these two models.

Previous studies performed on the wings of the dragonfly *Sympetrum vulgatum* showed that the thickness of the wing membranes changes between 3.6 and 15 μm [19]. In our models, the thickness of the membrane was assumed to be constant over the entire wing structure and equal to the value of about 5 μm [11, 18, 21, 30]. Wing veins were modelled as having a rectangular cross section. Considering the fact that veins in the insect wings are mainly dumbbell- or elliptical-shaped, their thickness in the models was adjusted to achieve the same mechanical effect. For this purpose, the thickness of the veins was assumed to be dependent on loading conditions. For example, when the wing model was under tensile stress, the thickness of the veins was adapted to make the same cross-sectional area as a real wing. Subsequently, when the model was under bending or torsion, the vein thickness was adjusted to produce the same moment of inertia and polar moment of inertia as the original wing sample, respectively. Eight sections along the wings were used for this adjustment procedure.

2.4 Material properties

Very limited data are available on the mechanical characteristics of dragonfly wing and its components [38, 40, 47], and we used them to complete our models. The measurement and investigation of the mentioned characteristics are out of the scope of this research. Therefore, in our simulations, the wing veins and membrane were assumed as homogeneous materials.

Previous experiments revealed that up to the fracture point, the wing material of locusts and dragonflies behaves in an elastic manner [14, 29]. Therefore, the wing veins and membranes were modelled as linear elastic materials with Young's moduli of 6 and 3.5 GPa, respectively [18]. The Poisson's ratio and density of both veins and membranes were considered to be 0.3 and 1200 kg m^{-3} , respectively [43].

2.5 Loadings and boundary conditions

Free vibration analysis was performed to measure the natural frequencies of the models and to identify their natural vibration modes. Recent studies indicated that both linear and nonlinear analyses yielded similar results [19]. Therefore, in order to decrease the computational costs, the vibration analysis was performed based on the assumption of geometric linearity.

The mechanical behaviour of the models was also studied under three different loading types including tension, bending and torsion. These loading conditions might differ from the typical loading condition that an insect wing experiences during normal flight. However, the external

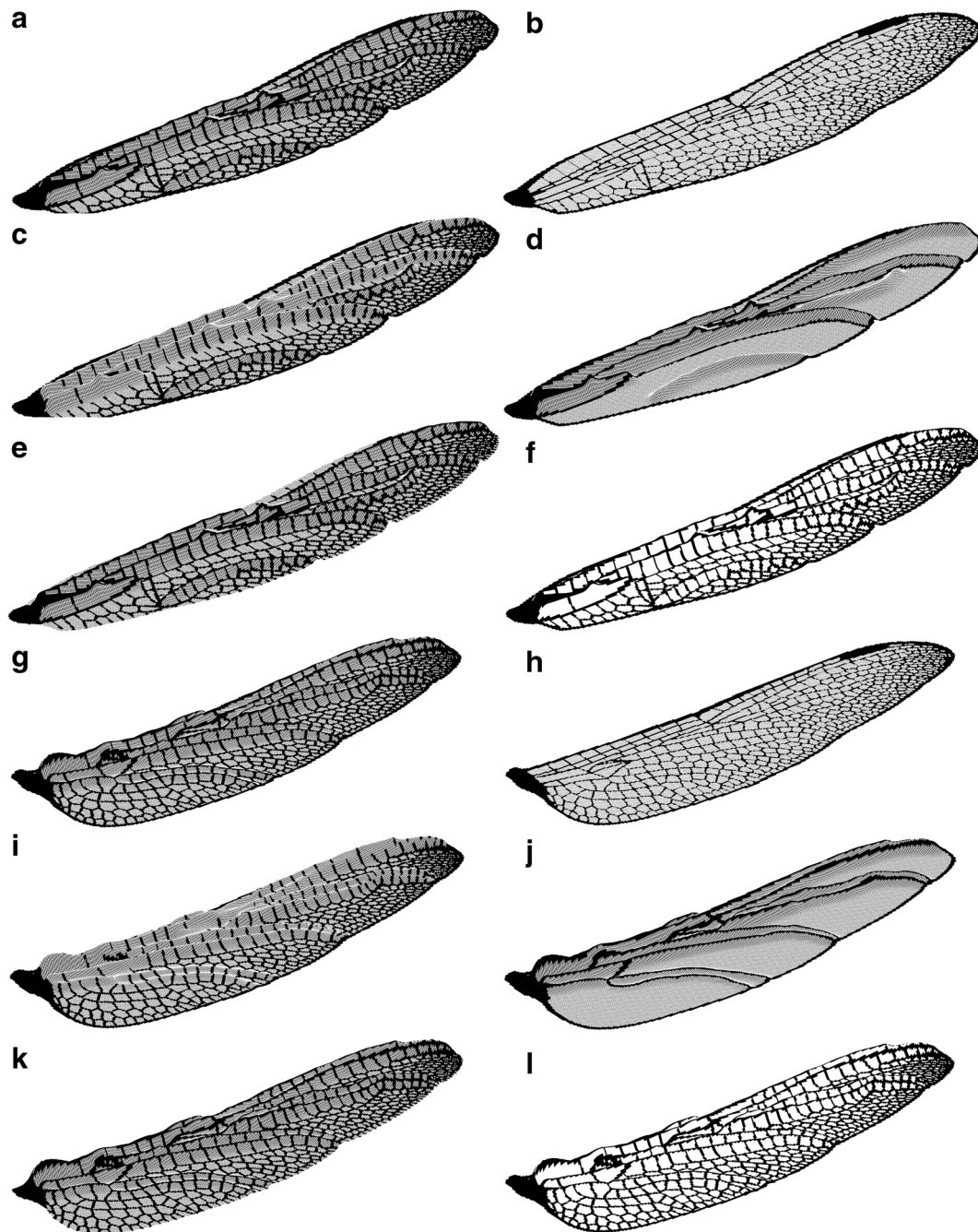


Fig. 2 FE models of the dragonfly wings. Models of the forewing: **a** model F1, **b** model F2, **c** model F3, **d** model F4, **e** model F5, **f** model F6 and models of hind-wing: **g** model H1, **h** model H2,

i model H3, **j** model H4, **k** model H5, **l** model H6. Detailed characteristics of the models are listed in Table 1

forces applied to the wings are supposed to be a combination of these three general loading types. Therefore, as the main objective of this study is to establish a comparative study between the mechanical behaviour of the models, these simplifications seem to be justified for this FE model trial.

Considering the assumption of linear elastic material behaviour, the deformation of the models should not

exceed the elastic limit (less than 5 % of the length of the models). Therefore, the magnitude of the applied forces in each loading condition was chosen accordingly.

Based on our previous experiments on the tensile properties of dragonfly wings [29], we chose a force of 0.5 N to produce a tensile force in the wing's spanwise direction. In order to simulate an experimental tensile test and to produce a uniform displacement distribution, this

Table 1 Characteristics of the models of dragonfly wings

Forewing/hind-wing	Membrane	Ambient veins	Longitudinal veins	Cross-veins	Corrugations
F1/H1	X	X	X	X	X
F2/H2	X	X	X	X	
F3/H3	X	X		X	X
F4/H4	X	X	X		X
F5/H5	X		X	X	X
F6/H6		X	X	X	X

force was applied to a rectangular frame (as the grips of a tensile machine) that held the wing [14].

Numerical simulation of bending was achieved by applying a point load of 0.5×10^{-3} N perpendicular to the wing surface and in downward direction. The magnitude of this force is 1/5 of the mean vertical force applied to the wings of dragonfly *Sympetrum frequens* in the steady slow climbing flight [2]. The load was imposed on the torsional axis of the wing that is necessary to prevent torsional deformations.

A 50×10^{-6} Nm torsional moment was used to make an angular deflection. The moment is produced around the torsional axis of the wings reported in Sunada et al. [41]. The value of the angular displacement was measured around this torsional axis. In all loading conditions, the models were considered to have a clamped boundary at the wing joint [21].

2.6 Mesh optimization

The accuracy of the results in a FE analysis depends on finding the coarsest mesh size that leads to a reasonable error tolerance. Therefore, a mesh convergence analysis was conducted by subdividing the mesh size of the models and solving the problem until reaching the results that are not dependent on the mesh size. Taking into account that the optimum mesh size depends on both the geometry of the model and the loading type, different mesh densities were obtained for each model in each analysis. An average element size of $0.09 \text{ mm} \times 0.09 \text{ mm}$ was found to be sufficient for an accurate numerical solution.

3 Results

3.1 Natural frequencies and mode shapes

The results from the vibrational analysis of the models are illustrated in Table 2. The numerically calculated values of the natural frequencies obtained from models F1 and H1 (the exact models of fore- and hind-wings, respectively) are in a very good agreement with the previous experimental results reported by the other researchers [4, 48]. The results

indicate that the first natural frequencies of the fore- and hind-wings are 151 and 146 Hz, respectively. The estimated values of the second and third natural frequencies are 295 and 530 Hz for the forewing, and 287 and 735 Hz for the hind-wing, respectively.

As seen in Table 2, the main deformation mechanism of the forewing models (models F1–F6) in the first vibration mode is bending that occurs at the tip of the wing near the trailing edge. The second natural vibration mode is dominated by torsion. The maximum torsional deformation takes place at a part of the leading edge close to the tip as well as the middle of the trailing edge. The results also indicate that the torsional deformation dominates the third mode. The magnitude of the deformation is much larger at the tip of the wing and middle of the trailing edge than the other parts. Almost the same types of deformation were observed for the hind-wing models (models H1–H6) in each fundamental natural mode. With an exception of one case (third mode shape of the model H4), there is no substantial difference between the fundamental mode shapes of fore- and hind-wings. There is a good correlation between the predicted numerical mode shapes and those previously observed by Chen et al. [4].

Figure 3 shows a comparison between the first three natural frequencies of the 12 developed models. Comparison of the results showed that removal of each constructional element significantly changes the wings' natural frequencies. For example, removal of corrugations (F2), longitudinal veins (F3), ambient veins (F5) and membranes (F6) decreases the first natural frequency of the forewing by 74, 56, 33 and 30 %, respectively. The first natural frequencies of hind-wing models with no corrugation (H2), longitudinal vein (H3), ambient vein (H5) and membrane (H6) are, respectively, 71, 49, 40 and 20 % less than the complete hind-wing model (H1). However, excluding the cross-veins (models F4 and H4) causes an increase in the fundamental natural frequencies of both wings by 19 and 30 %, respectively.

3.2 Loadings and deformations

Figure 4 presents the force–displacement diagrams from numerical simulations of the uniaxial tensile test, described

Table 2 Results of the numerical simulations

Model no.	Mode no.	Frequency (Hz)	Dominant mode shape	Location of maximum deformation					
				Leading edge close to the tip and middle of the trailing edge	Tip of the wing and middle of the trailing edge	Tip of the wing	Middle of the leading edge and trailing edge close to the tip	End and middle of the trailing edge	Camber near wing root
F1	1	151.04	Bending			X			
	2	295.35	Torsion	X					
	3	529.99	Torsion		X				
F2	1	38.93	Bending			X			
	2	222.25	Torsion	X					
	3	332.29	Torsion				X		
F3	1	66.62	Bending			X			
	2	180.95	Torsion	X					
	3	316.74	Torsion		X				
F4	1	179.06	Bending			X			
	2	274.08	Torsion	X					
	3	564.41	Torsion					X	
F5	1	101.84	Bending			X			
	2	238.31	Torsion	X					
	3	355.74	Torsion	X					
F6	1	105.63	Bending		X				
	2	236.91	Torsion	X					
	3	340.24	Torsion	X					
H1	1	146.40	Bending			X			
	2	287.04	Torsion	X					
	3	734.56	Torsion		X				
H2	1	42.71	Bending			X			
	2	214.68	Torsion	X					
	3	346.51	Torsion				X		
H3	1	74.58	Bending			X			
	2	199.54	Torsion	X					
	3	486.78	Torsion				X		
H4	1	189.60	Bending			X			
	2	298.79	Torsion	X					
	3	551.88	Bending						X
H5	1	88.27	Bending			X			
	2	267.24	Torsion		X				
	3	424.61	Torsion			X			
H6	1	117.30	Bending			X			
	2	237.96	Torsion	X					
	3	446.91	Torsion			X			

Comparison of the natural frequencies, mode shapes and location of the maximum deformations between the dragonfly wing models. To minimize rounding errors, all results of numerical calculations are reported with two significant figures

in Sect. 2.6. The resulting maximum principal stress distributions are also given in this figure and are plotted with the same contour legend. The elastic elongation of 83.2 μm obtained for the forewing model (F1) under a tensile load of 0.5 N is consistent with the results of our previous experiments [29] showing an average elongation of

86.0 μm for eleven samples of *O. sabina* dragonfly forewing.

As seen in Fig. 4, removing the constructional elements from the insect wings strongly influences their mechanical behaviour under tensile loading condition. Based on the simulation results, deletion of corrugations (models F2 and

Fig. 3 First three natural frequencies of the wing models

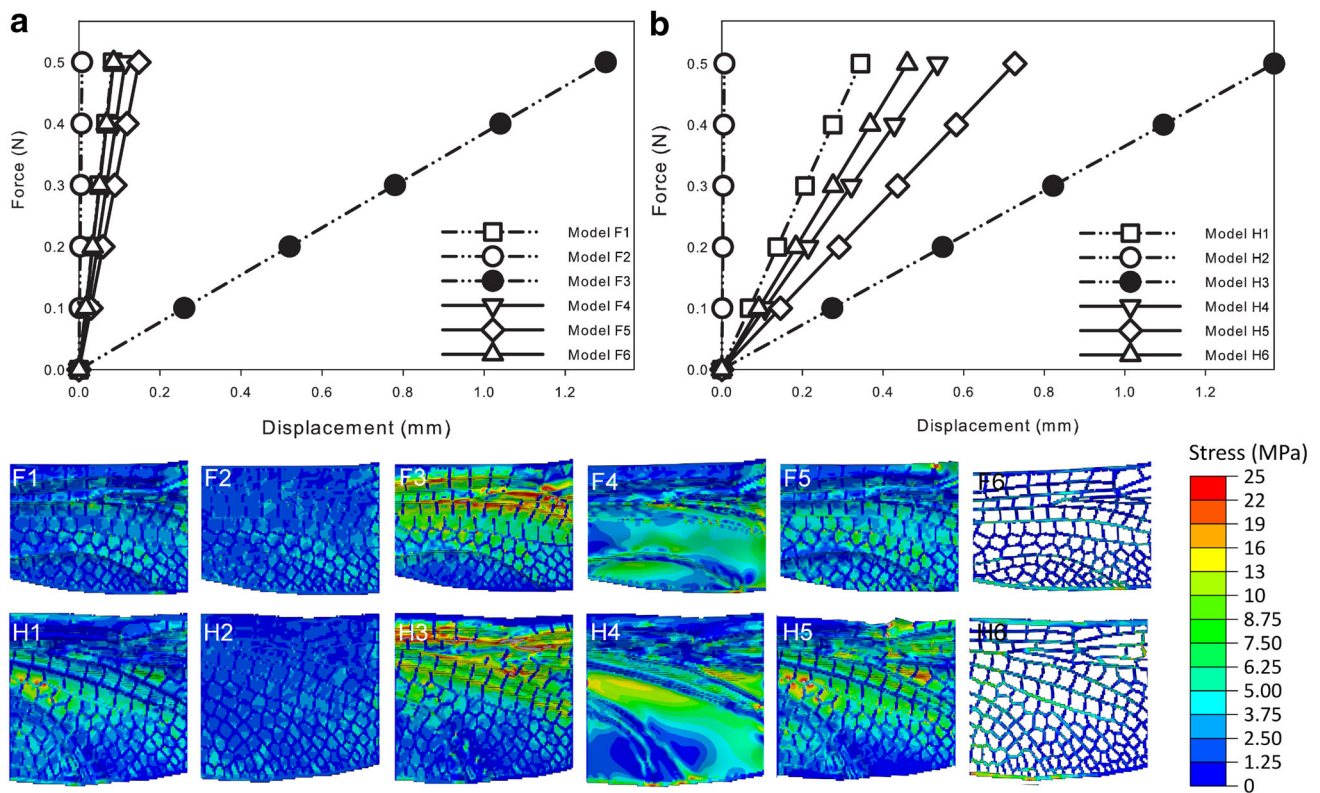
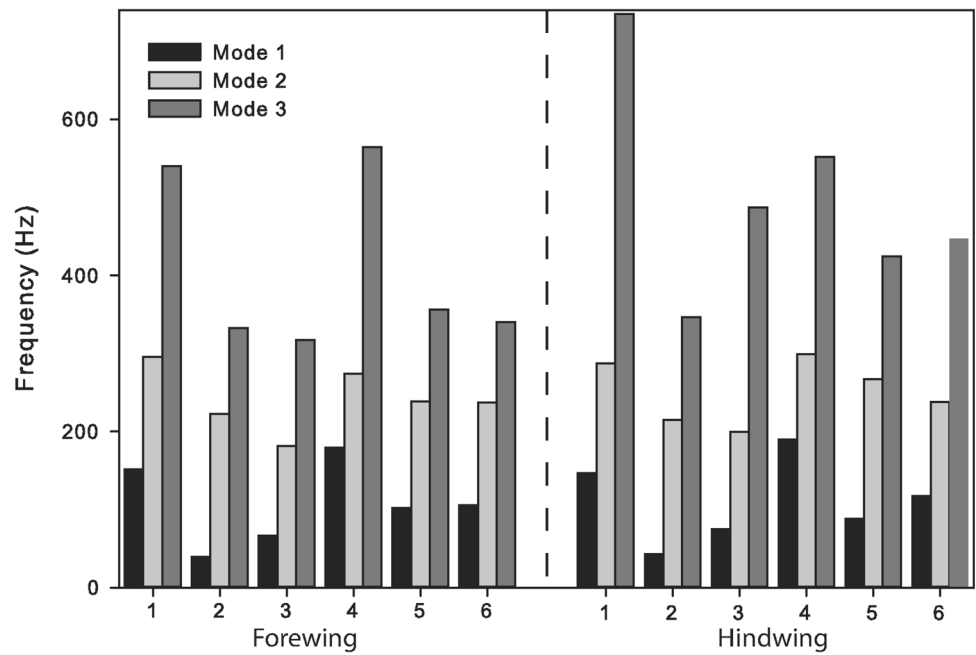


Fig. 4 Numerical force–displacement diagrams for **a** forewing and **b** hind-wing models under tension. The distribution of the maximum principal stress has been shown for all models. *Red colours* show the local stress concentrations

H2) leads to an increase in the axial rigidity of both wings. The removal of the longitudinal veins (models F3 and H3) produces a decrease in the axial stiffness, but it also causes high stress concentrations especially on the anterior part of

the wings. We found that the elimination of cross-veins (models F4 and H4) reduces the axial stiffness of the fore- and hind-wings by 27 and 36 %, respectively. It is important to note that, in this case, we observed relatively

higher stresses (1.7 times) in the membranes. By removing the ambient veins (models F5 and H5), the stiffness of fore- and hind-wings is decreased by 44 and 53 %, respectively. Deleting the membranes (model F6 and H6) yields a relatively small reduction in the axial rigidity of the forewing (around 3 %) but a larger decrease in the stiffness of the hind-wing. In this case, the values of the maximum stress in these two models (F6 and H6) are 1.3 and 1.1 times higher than the complete fore- and hind-wing models (F1 and H1), respectively.

Figures 5 and 6 represent the deflection of the models subjected to pure bending. The same contour legends are used in these two figures. The maximum deformations of the main wing models (F1 and H1), under the described loading condition, are 82.0 and 86.1 μm , respectively. These numerical results are in good agreement with the values obtained from the analytical equation that is used to calculate the deflection of a cantilever beam (81.5 and 88.2 μm for fore- and hind-wings, respectively). In this calculation, the flexural stiffness of the wings is supposed to be constant and equal to the average values of 6.2×10^{-5} and 6.3×10^{-5} N m^2 for fore- and hind-wings, respectively [23, 41].

We observed a very large increase in the maximum bending deformation of the models with no corrugation (models F2 and H2), in comparison with the complete wing models (models F1 and H1), by 18.4 and 15.4 times, respectively. Removal of the longitudinal veins (F3), cross-veins (F4) and ambient veins (F5) has a less effect and causes 5.8, 2.0 and 2.5 times increase in the bending deformation of the forewing, respectively. Although excluding the membrane from the forewing (model F6) leads to the less strong increase in deflection, the maximum deformation of this model is still 2.0 times larger than the respective deformation of the exact model of native forewing (model F1). Almost the same effects were observed in the deformation of the hind-wing by removing the same constructional elements.

The effect of the constructional elements on the angular displacement of the models due to a torsional moment is shown in Fig. 7. As displayed in this figure, removing each of these elements from the forewing implies an increase in the angular deformation of the main forewing model (F1). The results are qualitatively the same for the hind-wing model (H1). The maximum angles of twist of the models F1 and H1 subjected to the same twisting moment are 1.15° and 0.73° , respectively. The numerical data indicate that cross-veins have the most and membranes the least influences on the torsional rigidity of the dragonfly wings (Table 3). Interestingly, the effect of longitudinal veins on the torsional rigidity of the wings is very close to that of cross-veins.

Table 3 summarizes the effect of removal of each constructional element on the axial, bending and torsional rigidities of the insect fore- and hind-wings. The data are expressed in percent compared to the results obtained from the complete wing models (F1 and H1).

4 Discussion

4.1 The influence of the constructional elements on the natural frequencies and mode shapes of dragonfly wings

The effect of damping was not considered in our simulations. However, structural and aerodynamic damping may influence the natural frequencies of the wings. The following equation can be used to calculate the damped natural frequency of the wing system [32]:

$$\omega_d = \sqrt{1 - \zeta^2} \omega_n \quad (1)$$

where ω_d and ω_n are the damped and undamped natural frequencies, respectively, and ζ is the dimensionless damping ratio.

It has been demonstrated that the dragonfly wing structure and its surrounding air together provide an average damping ratio less than 5 % which cannot make a significant change in the dominant natural frequency and mode shapes [4, 7]. Therefore, considering a damping ratio of 5 % decreases the first natural frequencies of fore- and hind-wings to 150.85 and 146.22 Hz, respectively.

It has been previously reported that dragonflies flap their wings with a frequency between 29 and 52 Hz [24, 27, 36]. It means that the flapping frequency of these insects is at least 2.8 times and at most 5.2 times less than the resonance frequency of their wings. The considerable difference between the flapping and natural frequencies provides a safe and stable flight, as the morphology of the wing prevents it to vibrate at its natural frequency, and therefore avoids the flight disturbance and possible failure due to resonance.

The significant reduction in the first three natural frequencies of the wings due to the removal of corrugations (see Fig. 3) can be used to explain the empirical findings indicating the lower flapping frequency of damselfly wings than that of the wings of dragonflies [37]. The previous observations demonstrated that the maximum wing beat frequency of dragonflies, which belongs to *Epiophlebia superstes*, is around 52 Hz, whereas damselflies flap their wings with a maximum frequency of about 33 Hz. Based on our simulations, this difference may come from the more corrugated pattern of dragonfly wings compared to wings of damselflies.

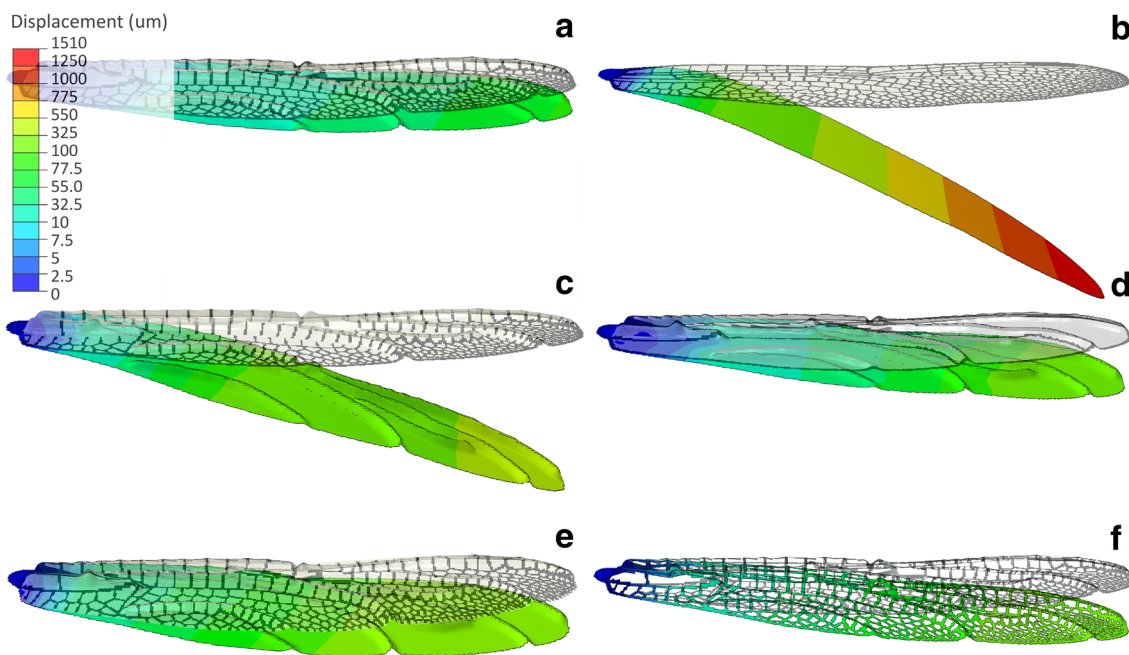


Fig. 5 Results of bending tests on FE models of the forewing. **a** Model F1, **b** model F2, **c** model F3, **d** model F4, **e** model F5 and **f** model F6. Detailed characteristics of the models are listed in Table 1

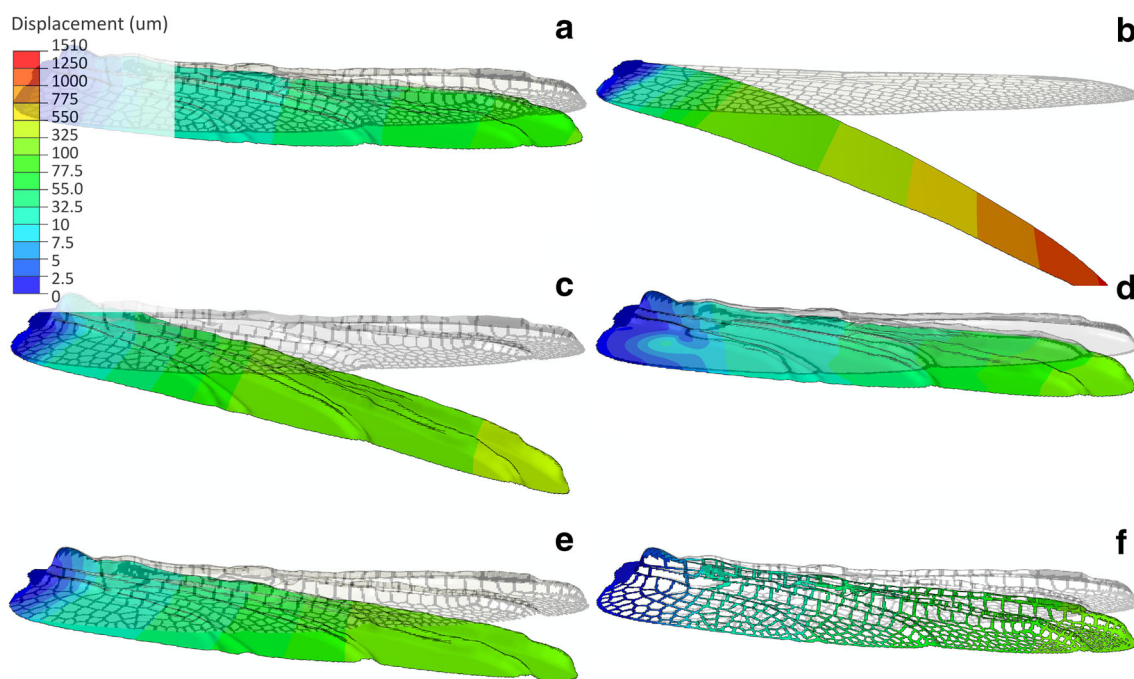


Fig. 6 Results of bending tests on FE models of the hind-wing. **a** Model H1, **b** model H2, **c** model H3, **d** model H4, **e** model H5 and **f** model H6. Detailed characteristics of the models are listed in Table 1

As clearly illustrated in Fig. 3, in contrast to the removal of the other constructional elements, removing cross-veins has an opposite effect and leads to an increase in the natural frequency of both fore- and hind-wings. This phenomenon is probably due to the fact that

cross-veins might affect the weight of the wing more than its overall stiffness. However, as recently reported, cross-veins in insect wings play an important role to distribute the stress and prevent stress concentrations [8].

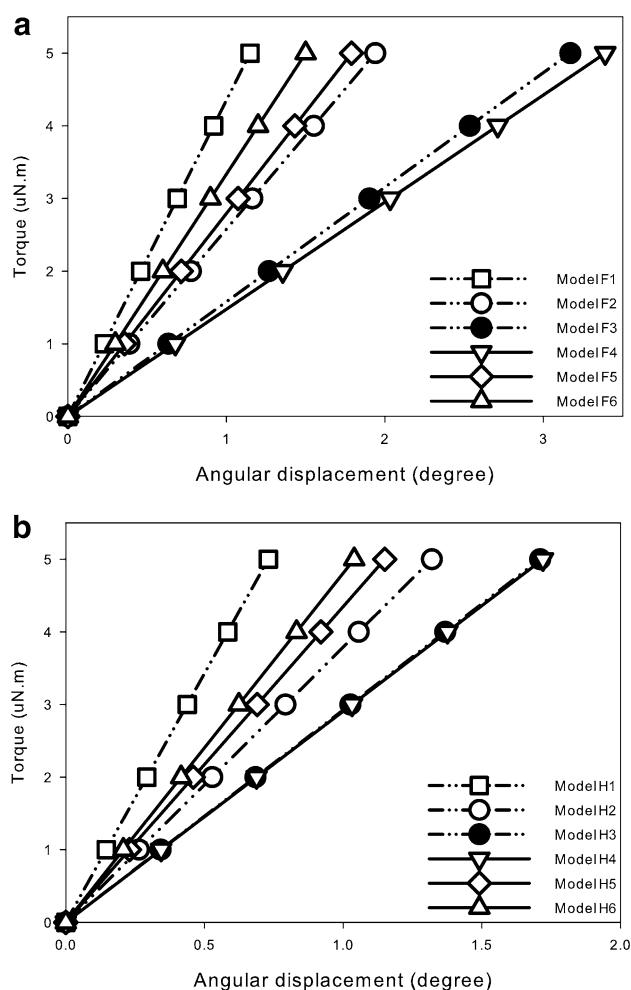


Fig. 7 Torque–angular displacement diagrams for **a** forewing and **b** hind-wing models

Further investigation of the results from modal analysis of the models revealed that the absence of a constructional element, just in one case (third mode shape of model H4), has no effect on their dominant form of deformation, and it has a small effect on the location of the maximal deformations (see Table 2). Indeed, the excessive oscillations induced by resonance mainly occur at the tip and trailing edge which are thinner and therefore more flexible than the other parts of the wings. However, removing one of the constructional elements from the complete models of the wings (models F1 and H1) may lead to a considerable increase in the magnitude of the deflection, especially when corrugations are missing from the wings.

4.2 The influence of the constructional elements on the axial stiffness of dragonfly wings

The remarkable difference in the deformation and stress distribution of the wing models subjected to tension suggests that the mechanical behaviour of the insect wings

under normal stresses in the spanwise direction is considerably affected by the interaction of all the constructional elements. Investigation of the stress distribution in the models with no longitudinal vein (models F3 and H3) and no cross-vein (models F4 and H4) compared to that of the main wing models (F1 and H1) shows high local stress concentrations on the anterior and posterior parts of the wings, respectively (see Fig. 4). Further, removal of ambient veins (models F5 and H5) from the margin of the wings increases the average tensile stress in whole wing structure. These results demonstrate the importance of the interaction between the wing veins in distributing stress and preventing stress concentrations, as observed in our previous simulations [8, 31]. Nevertheless, these stress concentrations may significantly decrease the load-bearing capacity of both wings.

Although, in comparison with the other constructional elements, the membrane has the lowest influence on the mechanical behaviour of the wing, removing the membrane from the wings considerably increases the stress levels in the veins. On the other hand, the models with no membrane (models F6 and H6) exhibit lower stiffness in comparison to the complete wing models (models F1 and H1). These results support the conclusion reached by Newman and Wootton [26] and Wootton et al. [46], indicating that the membrane in insect wings acts as a “stressed skin” that withstands the applied stress and increases the stiffness of the wing structure.

4.3 The influence of the constructional elements on the bending stiffness of dragonfly wings

The same mechanical resistance of the similar fore- and hind-wing models (models with similar constructional elements) to bending indicates the same functional role of each element in both wings (see Figs. 5, 6). In other words, the same constructional elements have the same influence on the bending behaviour of the dragonfly fore- and hind-wings. After removal of the corrugations (models F2 and H2), both wings of the insect showed a large increase in the bending deformation. This phenomenon suggests the crucial role of corrugations in improving the flexural stiffness of the wings (see Table 3), as previously reported by Rees [33, 34]. Otherwise, the extremely large deformation of the wing under the same bending stress may reduce the aerodynamic force production in flight or lead to structural failure [5, 25].

In comparison with the models with no corrugation (models F2 and H2), the other wing models showed a relatively lower reduction in the bending stiffness (see Table 3). The resulting change in the stiffness of the models with no membrane (models F6 and H6) in contrast to the complete wing models (models F1 and H1) confirms

Table 3 Results of the numerical simulations

Constructional element	Wing	Change in the axial stiffness (%)	Change in the bending stiffness (%)	Change in the torsional stiffness (%)
Corrugation	Forewing	+986.16	-94.57	-40.72
	Hind-wing	+5202.00	-93.51	-44.70
Longitudinal vein	Forewing	-93.60	-82.74	-63.72
	Hind-wing	-74.81	-80.25	-57.31
Cross-vein	Forewing	-27.02	-50.90	-66.08
	Hind-wing	-35.68	-34.36	-57.56
Ambient vein	Forewing	-43.78	-59.41	-35.75
	Hind-wing	-52.66	-62.66	-36.52
Membrane	Forewing	-2.80	-49.69	-23.33
	Hind-wing	-25.20	-33.45	-29.81

The effect of the removal of constructional elements (in percent) on the axial stiffness, bending stiffness and torsional stiffness of dragonfly fore- and hind-wings in comparison to the complete wing model

the statement described in the previous section about the effective influence of the membrane on the stiffness of the insect wing.

4.4 The influence of the constructional elements on the torsional stiffness of dragonfly wings

Numerical results indicated that all the constructional elements considered in this study noticeably influence the torsional behaviour of dragonfly wings (see Fig. 7a, b). Between all these elements, cross-veins were found to have the largest effect on the wing torsional rigidity (see Table 3). Considering the primary importance of cross-veins as structural elements linking longitudinal veins, we might suggest that, in torsion, the veins tend to maintain the shape of the wing and resist angular deformation by restraining the deflection of longitudinal veins and their movements. As seen in Fig. 7, removing longitudinal veins has almost the same effect on the torsional stiffness of the wings as that caused by the removal of cross-veins. This result provides more evidence for the proposed mechanism enhancing the torsional rigidity of the insect wings that involves the interaction of longitudinal and cross-veins.

Comparison of the results obtained from the analysis of the complete wing models (models F1 and H1) and 2D models (models F2 and H2) indicates that the wing corrugations may also increase the torsional rigidity. It seems likely that the corrugated design is a morphological adaptation that enables insect wings to resist higher torsional moments [41].

The results indicate that the constructional elements provide a balance between the flexibility and load-bearing ability of the wings. Based on our results, to build the flapping wings for a micro-aerial vehicle (MAV), one can possibly remove the cross-veins because it has been proved that, except membranes that are crucial to prevent air

passage, they are not as effective as the other wing elements. However, our previous work has shown that the cross-veins are the main elements of the “crack barrier” mechanism of the wing structure [14, 31].

In this study, we investigated the deformation and the stress distribution of the wing models under static loads. These loading conditions are different from those applying to the insect wing during flight. Although the behaviour of the wings are different when they are subjected to time-varying distributed forces, the presented deformation and stress analysis results can be used to better understand the complex biomechanical behaviour of dragonfly wings. However, one should note that the repeated stresses acting on the insect wings may significantly influence the strength of the wing structure and its lifetime. Therefore, the challenge of the future work is to understand the influence of the constructional elements on the fatigue behaviour of insect wings.

5 Conclusions

This article presents the results of a comparative study on the effects of some constructional elements on the complex vibrational and mechanical behaviour of dragonfly wings. Our results show that each constructional element may have a stronger effect in one condition, but a lesser effect in another one. In some cases, the constructional elements may also produce different effects. Using extensive numerical simulations, we have shown that cross-veins decrease the main natural frequency of the wings, whereas the other constructional elements increase it. The corrugations were found to have the strongest impact on the natural frequencies. The axial and bending rigidity of the wings are mainly influenced by longitudinal veins and corrugations. However, the torsional deformation of the

insect wings is mostly affected by the interaction of both longitudinal and cross-veins. Interestingly, in all cases, membranes were found to have the lowest effect on the vibrational and mechanical behaviour of the wings. Based on the results, we can conclude that the constructional elements and their complex interactions considerably influence the deformation of the wings in flight. Considering the importance of passive deformability of insect wings on their flight performance, the results obtained in this article may be useful in the future design of more efficient MAVs with bioinspired wing structures.

Acknowledgments This study was financially supported by German Academic Exchange Service (DAAD) to HR (Grant Number: 91524738-57048249) and the Max Planck Society.

Compliance with ethical standards

Conflicts of interest statement The authors declare there are no conflicts of interest to disclose.

References

1. A. Azuma, T. Watanabe, Flight performance of a dragonfly. *J. Exp. Biol.* **137**(1), 221–252 (1988)
2. A. Azuma, S. Azuma, I. Watanabe, T. Furuta, Flight mechanics of a dragonfly. *J. Exp. Biol.* **116**(1), 79–107 (1985)
3. T.M. Broering, Y. Lian, W. Henshaw, Numerical investigation of energy extraction in a tandem flapping wing configuration. *AIAA J.* **50**(11), 2295–2307 (2012)
4. J.S. Chen, J.Y. Chen, Y.F. Chou, On the natural frequencies and mode shapes of dragonfly wings. *J. Sound Vib.* **313**(3), 643–654 (2008)
5. P. Coffin, G. Ahmadi, R. Jha, P. Marzocca, Experimental In-flight rolling MAV wing deployment and aerodynamic characterization. *SAE Int. J. Aerosp* **4**, 1106–1114 (2011)
6. S.A. Combes, T.L. Daniel, Flexural stiffness in insect wings II. Spatial distribution and dynamic wing bending. *J. Exp. Biol.* **206**(17), 2989–2997 (2003)
7. S.A. Combes, T.L. Daniel, Into thin air: contributions of aerodynamic and inertial-elastic forces to wing bending in the hawkmoth *Manduca sexta*. *J. Exp. Biol.* **206**(17), 2999–3006 (2003)
8. A. Darvizeh, N. Shafiee, M. Darvizeh, H. Habibollahi, H. Rajabi, Investigation of the effects of constructional elements on the biomechanical behavior of desert locust hind wing. *Modares J Mech Eng* **14**(14), 235–244 (2015)
9. A. Darvizeh, H. Rajabi, A. Khasheshi, Biomechanical aspects of dragonfly wing composite structure. in *Presented at the International Bionic Engineering Conference*, Boston (2011a)
10. A. Darvizeh, H. Rajabi, A. Khasheshi, M.K. Sobhani, J. Etedadi, Morphological and numerical investigations of butterfly wing composite structure. in *Presented at the International Bionic Engineering Conference*, Boston (2011b)
11. M. Darvizeh, A. Darvizeh, H. Rajabi, A. Rezaei, Free vibration analysis of dragonfly wings using finite element method. *Int. J. Multiphys.* **3**(1), 101–110 (2009)
12. C. Dileo, X. Deng, Design of and experiments on a dragonfly-inspired robot. *Adv. Robot.* **23**(7–8), 1003–1021 (2009)
13. J.H. Dirks, D. Taylor, Fracture toughness of locust cuticle. *J. Exp. Biol.* **215**(9), 1502–1508 (2012)
14. J.H. Dirks, D. Taylor, Veins improve fracture toughness of insect wings. *PLoS ONE* **7**(8), e43411 (2012)
15. S. Eshghi, H. Rajabi, A. Darvizeh, V. Nooraefar, A. Shafiei, T.M. Mostofi, M. Monsef, A simple method for geometric modelling of biological structures using image processing technique. *Scientia Iranica* (in press)
16. N. Gaissert, R. Mugrauer, G. Mugrauer, A. Jebens, K. Jebens, E.M. Knubben, Inventing a micro aerial vehicle inspired by the mechanics of dragonfly flight. in *Towards Autonomous Robotic Systems*, ed. by A. Natraj, S. Cameron, C. Melhuish, M. Witkowski (Springer, Berlin, 2014), pp. 90–100
17. S.N. Gorb, A. Kesel, J. Berger, Microsculpture of the wing surface in Odonata: evidence for cuticular wax covering. *Arthropod Struct. Dev.* **29**(2), 129–135 (2000)
18. R.C. Herbert, P.G. Young, C.W. Smith, R.J. Wootton, K.E. Evans, The hind wing of the desert locust (*Schistocerca gregaria* Forskal). III. A finite element analysis of a deployable structure. *J. Exp. Biol.* **203**(19), 2945–2955 (2000)
19. S.R. Jongerius, D. Lentink, Structural analysis of a dragonfly wing. *Exp. Mech.* **50**(9), 1323–1334 (2010)
20. A.B. Kesel, Aerodynamic characteristics of dragonfly wing sections compared with technical aerofoils. *J. Exp. Biol.* **203**(20), 3125–3135 (2000)
21. A.B. Kesel, U. Philippi, W. Nachtigall, Biomechanical aspects of the insect wing: an analysis using the finite element method. *Comput. Biol. Med.* **28**(4), 423–437 (1998)
22. M. Lee, Dragonfly wings: special structures for aerial acrobatics. in *Remarkable Natural Material Surfaces and Their Engineering Potential* (Springer International Publishing, Switzerland, 2014), pp. 65–77
23. S. Mukherjee, R. Ganguli, A dragonfly inspired flapping wing actuated by electro active polymers. *Smart Struct. Syst.* **6**(7), 867–887 (2010)
24. H. Naka, Y. Sunami, H. Hashimoto, Development of the artificial wing suitable for flapping micro air vehicle based on dragonfly wing. The 3rd International Conference on Design Engineering and Science (ICDES 2014), Pilsen (2014)
25. T. Nakata, H. Liu, Aerodynamic performance of a hovering hawkmoth with flexible wings: a computational approach. *Proc. R. Soc. Lond. B Biol. Sci.* **279**(1729), 722–731 (2012)
26. D.J.S. Newman, R.J. Wootton, An approach to the mechanics of pleating in dragonfly wings. *J. Exp. Biol.* **125**(1), 361–372 (1986)
27. R.A. Norberg, Hovering flight of the dragonfly *Aeschna juncea* L., kinematics and aerodynamics. in *Swimming and Flying in Nature*, ed. by T.Y.-T. Wu, C.J. Brokaw, C. Brennen (Springer, New York, 1975), pp. 763–781
28. M. Okamoto, K. Yasuda, A. Azuma, Aerodynamic characteristics of the wings and body of a dragonfly. *J. Exp. Biol.* **199**(2), 281–294 (1996)
29. H. Rajabi, A. Darvizeh, Experimental investigations of the functional morphology of dragonfly wings. *Chin. Phys. B* **22**(8), 088702 (2013)
30. H. Rajabi, M. Moghadami, A. Darvizeh, Investigation of microstructure, natural frequencies and vibration modes of dragonfly wing. *J. Bionic Eng.* **8**(2), 165–173 (2011)
31. H. Rajabi, A. Darvizeh, A. Shafiei, D. Taylor, J.H. Dirks, Numerical investigation of insect wing fracture behaviour. *J. Biomech.* **48**(1), 89–94 (2015)
32. S.S. Rao, F.F. Yap, *Mechanical Vibrations*, vol. 4 (Addison-Wesley, New York, 1995)
33. C.J. Rees, Form and function in corrugated insect wings. *Nature* **256**, 200–203 (1975)
34. C.J. Rees, Aerodynamic properties of an insect wing section and a smooth aerofoil compare. *Nature* **258**, 141–142 (1975)

35. H.H. Ren, X.S. Wang, Y.L. Chen, X.D. Li, Biomechanical behaviors of dragonfly wing: relationship between configuration and deformation. *Chin. Phys. B* **21**(3), 034501 (2012)
36. G. Rüppell, Kinematic analysis of symmetrical flight manoeuvres of Odonata. *J. Exp. Biol.* **144**(1), 13–42 (1989)
37. G. Rüppell, D. Hilfert, The flight of the relict dragonfly *Epiophlebia superstes* (Selys) in comparison with that of the modern Odonata (Anisozygoptera: Epiophlebiidae). *Odonatologica* **22**(3), 295–309 (1993)
38. F. Song, K.W. Xiao, K. Bai, Y.L. Bai, Microstructure and nanomechanical properties of the wing membrane of dragonfly. *Mater. Sci. Eng., A* **457**(1), 254–260 (2007)
39. S. Sudo, K. Tsuyuki, T. Ikohagi, F. Ohta, S. Shida, J. Tani, A study on the wing structure and flapping behavior of a dragonfly. *Int. J. Ser. C Mech. Syst. Mach. Elem. Manuf.* **42**(3), 721–729 (1999)
40. J.Y. Sun, C.X. Pan, J. Tong, J. Zhang, Coupled model analysis of the structure and nano-mechanical properties of dragonfly wings. *Nanobiotechnology IET* **4**(1), 10–18 (2010)
41. S. Sunada, L. Zeng, K. Kawachi, The relationship between dragonfly wing structure and torsional deformation. *J. Theor. Biol.* **193**(1), 39–45 (1998)
42. M. Vanella, T. Fitzgerald, S. Preidikman, E. Balaras, B. Balachandran, Influence of flexibility on the aerodynamic performance of a hovering wing. *J. Exp. Biol.* **212**(1), 95–105 (2009)
43. J.F. Vincent, U.G. Wegst, Design and mechanical properties of insect cuticle. *Arthropod Struct. Dev.* **33**(3), 187–199 (2004)
44. J.M. Wakeling, C.P. Ellington, Dragonfly flight. III. Lift and power requirements. *J. Exp. Biol.* **200**(3), 583–600 (1997)
45. R.J. Wootton, Functional morphology of insect wings. *Annu. Rev. Entomol.* **37**(1), 113–140 (1992)
46. R.J. Wootton, K.E. Evans, R. Herbert, C.W. Smith, The hind wing of the desert locust (*Schistocerca gregaria* Forskal). I. Functional morphology and mode of operation. *J. Exp. Biol.* **203**(19), 2921–2931 (2000)
47. K. Xiao, K. Bai, W. Wang, F. Song, Experimental study on the microstructure and nanomechanical properties of the wing membrane of dragonfly. *Acta. Mech. Sin.* **23**(3), 281–285 (2007)
48. L. Zeng, H. Matsumoto, S. Sunada, T. Ohnuki, K. Kawachi, Two-dimensional, noncontact measurement of the natural frequencies of dragonfly wings using a quadrant position sensor. *Opt. Eng.* **34**(4), 1226–1231 (1995)